**Real-time cell cycle imaging in a 3D cell culture model of melanoma**

Loredana Spoerri[1*], Kimberley A. Beaumont[2,3*], Andrea Anfosso[2,3], Nikolas K. Haass[1,2,4]

[1]The University of Queensland, The University of Queensland Diamantina Institute, Translational Research Institute, Brisbane, Qld, Australia

[2]The Centenary Institute, Newtown, NSW, Australia

[3]Sydney Medical School, University of Sydney, NSW, Australia

[4]Discipline of Dermatology, University of Sydney, NSW, Australia.

[*]these authors contributed equally to this work

**Correspondence:**

Nikolas K. Haass, The University of Queensland Diamantina Institute, Translational Research Institute, 37 Kent St, Woolloongabba, Queensland 4102, Australia

Phone +61 7 3443 7087; fax +61 7 3443 6966; e-mail n.haass1@uq.edu.au

**Running head:** 3D real-time cell cycle imaging

**i. Summary/Abstract**

Aberrant cell cycle progression is a hallmark of solid tumors; therefore cell cycle analysis is an invaluable technique to study cancer cell biology. However, cell cycle progression has been most commonly assessed by methods that are limited to temporal snapshots or that lack spatial information. Here we describe a technique that allows spatiotemporal real-time tracking of cell cycle progression of individual cells in a multicellular context. The power of this system lies in the use of 3D melanoma spheroids generated from melanoma cells engineered with the fluorescent ubiquitination-based cell cycle indicator (FUCCI). This technique allows us to gain further and more detailed insight into several relevant aspects of solid cancer cell biology, such as tumor growth, proliferation, invasion and drug sensitivity.

**ii. Key words:** fluorescent ubiquitination-based cell cycle indicator (FUCCI); real-time imaging; 3D spheroid; tumor heterogeneity; tumor microenvironment; cancer drug resistance; migration; invasion

## 1. Introduction

To understand cancer cell biology, especially the process of metastasis, it is necessary to assess the proliferative and invasive behavior in the context of the location within the tumor and its complex microenvironment (1,2). In comparison to 2D cell culture models, *in vitro* 3D tumor models mirror *in vivo* tumor biology and drug response more faithfully (3-5). They are therefore an important tool in the field of cancer research and a good compromise between the lack of a microenvironment encountered under 2D culture conditions and the great complexity of *in vivo* animal models.

Within the range of available *in vitro* 3D tumor models, spheroids present the advantage of being the relatively quickest and technically simplest method to recapitulate multiple characteristics of solid tumors at once: Spheroids mimic physiological tumor behavior in terms of growth, proliferation, invasion, cell-cell and cell-matrix interactions, molecule diffusion, oxygen/nutrient gradients – with a hypoxic zone and a central necrosis – as well as drug sensitivity (3,5). Spheroids can be generated from cell lines but also from primary patient-derived cells (6).

Since uncontrolled proliferation is a hallmark of malignancies (7,8), understanding cell cycle behavior in detail is crucial in cancer research. Quantitation of DNA content by flow cytometry of cells stained with fluorescent markers and DNA pulse incorporation and detection of nucleotide analogues are probably the most commonly used techniques for cell cycle analysis. Even though the latter approach provides some chronological insight into the studied process, both methods provide information limited to snapshots taken at specific time points. However, cell cycle analysis has been recently revolutionized by a new method: fluorescent ubiquitination-based cell-cycle indicator (FUCCI) (9). This genetically encoded system allows spatial and temporal real-time tracking of cell cycle progression of individual cells in a multicellular context. The FUCCI technology is based on the overexpression of two modified cell cycle dependent proteins, Geminin and Cdt1, each respectively fused to the green and red fluorescence emitting proteins Azami Green [mAG-hGem(1-110)] and monomeric Kusabira Orange 2 [mKO2-hCdt1(30-120)]. Synthesis and degradation of Cdt1 and Geminin during cell cycle progression results in the nucleus of FUCCI-expressing cells to appear red in $G_1$ phase, yellow in early S phase and green in late S, $G_2$ and M phase. Immediately following cytokinesis and for a brief period of time at the very beginning of $G_1$ phase the cell nucleus does not display any fluorescence.

We have incorporated this real-time cell cycle tracking system in to a melanoma 3D *in vitro* model by generating spheroids initiated from FUCCI melanoma cell lines (10). We have used this system to study dynamic heterogeneity in cell cycle behavior and invasion (10), drug sensitivity (11) and acquired multidrug tolerance in melanoma (12). We have demonstrated the presence and specific distribution of sub-compartments of cells with different cell cycle behavior. More specifically, cycling cells were found in the spheroid periphery, while $G_1$-arrested cells located in more internal zones. This specific distribution correlated with oxygen and nutrient accessibility. These characteristics reflected those observed *in vivo* in mouse xenograft tumors generated from corresponding FUCCI melanoma cell lines, confirming the physiological relevance of this *in vitro* cell based model. Furthermore, we showed that invading cells are actively cycling and that cells arrested in $G_1$, due to their specific location within the spheroid or to drug treatment, were able to resume proliferation and invasion when re-exposed to the same favorable conditions experienced by the cycling cells (10).

The method described in this chapter allows us to study the spatiotemporal cell cycle dynamics of individual cells within the 3D structure of spheroids in real time, and therefore to gain insight into cancer relevant processes such as proliferation and invasion (13). Briefly, cultured melanoma cells are transduced with the FUCCI cell cycle indicator system. The red and green double-positive cells are isolated by fluorescence-activated cell sorting in order to obtain optimal and comparable fluorescence intensity of both the green and red fluorescence. Spheroids are then generated using these cells based on a non-adherent surface method (5,14), embedded in a collagen matrix and their individual cell behavior monitored by confocal fluorescent time-lapse microscopy. 3D reconstruction of FUCCI cell distribution in spheroids can be performed using multiphoton microscopy and 3D stitching. The physical separation of the tumor sub-compartments by Hoechst dye diffusion and subsequent

fluorescence-activated cell sorting has been described recently (10,14) and is beyond the scope of this methods chapter.

## 2. Materials

### 2.1 Generation of FUCCI expressing melanoma cell lines

1. $CO_2$ incubator.
2. 6-well and 96-well plates.
3. HEK293T cells and the melanoma cell line(s) of choice to be transduced.
4. Distilled $H_2O$ ($dH_2O$) and Milli-Q $H_2O$ (MQ $H_2O$).
5. Trypsinization solution: 0.05% Trypsin, 0.5 mM EDTA in PBS without $Ca^{2+}$ and $Mg^{2+}$.
6. HEK293T medium: 10% fetal bovine serum (FBS) in Dulbecco's Modified Eagle Medium.
7. Melanoma cell medium ("Tu4% medium"): 80% MCDB-153 medium, 20% L-15 medium (Leibovitz), 4% FBS, 5 µg/mL insulin, 1.68 mM $CaCl_2$. Dissolve the whole content of an MCDB-153 vial (17.6 g of powder) in 800 mL deionized $H_2O$, add 15.7 mL of 7.5% sodium bicarbonate, adjust pH to 7.2-7.4 using NaOH pellets or concentrated NaOH (see **Note 1**) and top up with deionized $H_2O$ to 1 L. Filter sterilize using a 0.2 µm filter, remove 200 mL, add 200 mL of L-15 medium (Leibovitz), 40 mL of FBS, 500 µL of 10 mg/mL insulin and 1120 µL of 1.5 M $CaCl_2$.
8. FUCCI constructs: mKO2-hCdt1 (30-120) and mAG-hGem (1-110) (9), sub-cloned into a replication-defective, self-inactivating lentiviral expression vector system (15).
9. Lentiviral vectors: pMDLg/pRRE, pRSV-Rev and pCMV-VSV-G (15).

10. 2× HeBS (HEPES buffered saline): 50 mM HEPES, 10 mM KCl, 12 mM Dextrose, 280 mM NaCl, 1.5 mM $Na_2HPO_4$. Adjust to pH 7.1. Filter with a 0.22 μm filter, aliquot and store at -20°C.
11. 2.5 M $CaCl_2$: To prepare 40 mL, dissolve 11.025 g of $CaCl_2$ in 30 mL of $dH_2O$. Filter with a 0.22 μm filter, aliquot and store at -20°C.
12. Sterile phosphate buffered solution (PBS): 137 mM NaCl, 2.7 mM KCl, 10 mM $Na_2HPO_4$, 1.8 mM $KH_2PO_4$ in $H_2O$.
13. Centrifuge.
14. 0.22 μm and 0.45 μm filters.
15. -80°C and -20°C freezer.
16. Polybrene, 100 mg/mL in sterile $H_2O$. Filter and store at -20°C.
17. Inverted fluorescence microscope.
18. Hemocytometer or automated cell counter.
19. Sorting medium 10% FBS in PBS.
20. FACSAria cell sorter.
21. Inverted phase-contrast microscope.

**2.2 Spheroid formation and embedding**

1. Well coating solution: 1.5% agarose in sterile PBS. Mix 0.45 g of tissue culture agarose in 30 mL of sterile PBS (see **Note 2**) and microwave until the agarose has completely dissolved (see **Note 3**). Prepare freshly before plate coating.
2. Trypsin neutralizing medium : 10% FBS in L-15 medium (Leibovitz).

3. Melanoma cell medium.
4. 200 mM L-Glutamine.
5. 10× Eagle's Minimum Essential Medium (EMEM).
6. Bovine type I collagen (R&D Systems), 5 mg/mL.
7. Fetal bovine serum (FBS).
8. 7.5% (w/v) $NaHCO_3$.
9. Sterile $dH_2O$.
10. 96-well plate.
11. Hemocytometer or automated cell counter.
12. $CO_2$ incubator.
13. Inverted phase-contrast microscope.

**2.3 FUCCI-spheroid imaging**

1. Time-lapse confocal microscope, e.g. Leica SPF confocal inverted microscope equipped with 8 laser lines and 5 filter-free PMT detectors (488 and 561 nm lasers to excite mAG and mKO2), low magnification and long working distance objectives (10× PL FLUOTAR objective (NA 0.3) or a 20x PL FLUOTAR objective (NA 0.5)) as well as an incubator chamber to maintain the standard cell culture conditions (i.e. humidity, 37°C and 5% $CO_2$).
2. Multiphoton microscope, e.g. a custom-built upright TriM Scope two-photon microscope (LaVision BioTec) equipped with a diode-pumped, wideband mode-locked Ti:Sapphire femtosecond laser (MaiTai, SpectraPhysics) and an APE Optical Parametric Oscillator (OPO), Photomultiplier tubes (Hamamatsu Photonics), 520 nm dichroic and bandpass

filter 560/40 (Chroma Technology) and a water-dipping 20× objective (Olympus XLUMPlanFL IR coated, NA 0.95).

3. Software: Imaris (Bitplane), Image J/Fiji (open source), Volocity (Perkin Elmer).

## 3. Methods

### 3.1 Transfection of HEK293T cells

1. Harvest exponentially growing HEK293T cells (see **Note 4**) the day before the transfection, centrifuge at 300 × g for 5 min, count and plate them in a 6-well plate so the cells will be 70% confluent the next day.
2. On the day of transfection, replace old medium with 2 mL of fresh medium 4 h before transfection.
3. Prepare 500 µL of calcium phosphate-DNA mix per each transfection in MQ $H_2O$. Co-transfect HEK293T cells with 0.5 µg each of the packaging defective helper construct (pMDLg/pRRE), the nuclear localization signal Rev plasmid (pRSV-Rev), a plasmid coding for a heterologous (pCMV-VSV-G) envelope protein, 8.5 µg of the vector construct harboring either mKO2-hCdt1 (30-120) or mAG-hGem (1-110) and 50 µL of 2.5 M $CaCl_2$.
4. Add 500 µL of the transfection solution drop by drop to 500 µL of the 2× HeBS solution while vortexing (see **Note 5**).
5. Let the solution stand at room temperature for 15 min, vortex every 5 min.
6. Slowly add the 1 mL of solution to each well while gently swirling the plate.
7. After 4 h remove the medium, wash with PBS, add fresh medium and incubate at 37°C, 5% $CO_2$.

8. After 48 h harvest the supernatant containing the lentiviral particles and centrifuge at 300 × g for 5 min (see **Note 6**).
9. Filter the supernatant with a 0.45 μm filter.
10. Aliquot in cryovials and store the supernatant at -80°C or proceed with the transduction of the melanoma cells (see **Note 7**).

### 3.2 Transduction of melanoma cells

1. Plate melanoma cell line in a 6-well plate so that they will be in the exponential grow phase during the transduction the next day (see **Notes 8-10**).
2. Replace old medium with 2 mL of fresh medium 4 h before transfection.
3. Thaw the lentiviral stock on ice.
4. Prepare the polybrene working solution at 8 mg/mL in culture medium.
5. Prepare 400 μL of transduction solution by mixing 200 μL of each FUCCI lentivirus (mKO2-hCdt1 (30-120) and mAG-hGem (1-110)) and add 0.4 μl of 8 mg/mL polybrene (final concentration of 8 μg/mL) (see **Notes 11** and **12**)
6. Add the transduction solution drop by drop while gently swirling the plate and return plate to the incubator.
7. After 72 h check the transduction efficiency under the fluorescence microscope.

### 3.3 Sorting of FUCCI-expressing single cell clones

1. Trypsinize melanoma cells in the exponential growth phase (see **Notes 8** and **13**).
2. Centrifuge at 300 × g for 5 min.

3. Remove the supernatant and count the cells.
4. Resuspend the cells in sorting medium at $1 \times 10^6$ cells/mL.
5. Using a FACSAria cell sorter, acquire using the 488 nm laser and the B530 detector for mAG, and B575 for mKO2.
6. Sort double positive cells, highly expressing mKO2-hCdt1 (30-120) and mAG-hGem (1-100) into a 96-well plate pre-filled with medium.
7. Check at the phase-contrast microscope that no more than one cell is present in each well (see **Note 14**).
8. Return to the incubator.
9. Check every day to spot the first dividing clones (see **Note 15**).
10. Trypsinize cells when confluent and split to a 24-well plate. Continue to expand cells until there are enough to freeze down in liquid nitrogen for further use.

### 3.4 Spheroid formation

1. To prepare one 96-well plate for spheroid formation, freshly prepare 30 mL of well coating solution and immediately dispense 100 µL of the solution in each well (see **Note 16**). Let the plate rest at room temperature for 15 min to allow the agarose to cool down and harden.
2. In the meantime, trypsinize the FUCCI-expressing cells (see **Note 17**): Wash the cells once with PBS and then treat with 0.05% Trypsin/EDTA for 5 min at 37°C.
3. Neutralize the trypsin by adding trypsin neutralizing medium and pipet repeatedly to create a single-cell suspension.

4. Centrifuge at 300 × g for 5 min.

5. Remove supernatant and resuspend the cells in cell culture medium.

6. Count the cells using a hemocytometer or an automatic cell counter and resuspend 600,000 cells in 24 mL of cell culture medium in order to obtain a solution at a concentration of $2.5 \times 10^4$ cells/mL.

7. Using a multichannel pipette add 200 µL of the cell suspension to each well so that 5000 cells are seeded per well (see **Note 18**).

8. Place the plate in the incubator for the following 72 h, allowing the spheroids to form (Fig. 1) (see **Note 19**).

9. Use a phase-contrast microscope to inspect the spheroids and mark the wells where the spheroids have formed properly (see **Note 20**).

[Fig. 1 near here]

**3.5 Spheroid embedding in collagen matrix**

1. To prepare 1 mL of the collagen embedding solution, mix 100 µL of 10X EMEM, 10 µL of 200 mM L-Glutamine and 400 µL of bovine type I collagen (see **Note 21** and **Note 22**). Work on ice (see **Note 23**).

2. Titrate the solution with 7.5% $NaHCO_3$ until the solution turns from a yellow-orange to a peach-pink color (the volume required for this change in pH should be around 15-30 µL).

3. Add 100 µL of FBS and top up to 1 mL with $H_2O$.

4. Mix well while taking care to avoid generating bubbles and keep on ice.

5. Add 40 µL in each well of a new flat bottom 96-well plate (see **Note 24**) and incubate plate for 5 min at 37°C to allow the collagen to polymerize (See **Note 25**).
6. Transfer spheroids from the 96-well plate where they have been cultured to sterile microcentrifuge tubes using a pipette and pipette tips with enlarged aperture (see **Note 26**). Transfer one spheroid per tube (Fig. 2) (see **Note 27**).
7. Let spheroids settle by gravity to the tube's bottom and remove the supernatant taking care to not disturb the spheroid (see **Note 28**).
8. Gently resuspend each spheroid in 60 µL of collagen solution (use pipette and pipette tips with enlarged aperture) and transfer into the 96-well plate that was previously coated with 40 µL per well of collagen solution (step 5).
9. Incubate plate for 15 min at 37°C to allow the collagen to polymerize.
10. With the use of a phase-contrast microscope inspect spheroid integrity and distribution in the well (if multiple spheroids were seeded per well).
11. Add 200 µL per well of appropriate medium and incubate at 37°C until the setup of the spheroid time-lapse confocal microscopy analysis.

[Fig. 2 near here]

### 3.6 FUCCI-spheroid time-lapse imaging using confocal microscopy

1. Set the microscope to a low magnification and turn on the laser to excite the Azami Green or Kusabira Orange 2 proteins (see **Note 29**).
2. Move to the well containing the spheroid to be imaged, locate the spheroid and center it in the field of view.

3. Set the microscope to a magnification that allows visualization of the whole spheroid (see **Note 30**).

4. Position the plane of view in the center of the spheroid (see **Note 31**). To do so, adjust the z variable starting with the view plane at the bottom of the spheroid then moving it deeper into the spheroid. During this process the diameter of the spheroid should increase until the center of the spheroid has been reached (see **Note 32**).

5. Adjust the necessary settings (exposure time, gain, laser power, etc.) to achieve optimal signal without overexposed zones.

6. Set up four optical slices on each side of the central plane, each separated by 5 µm. This results in a total of 9 optical slices (including the central slice) encompassing a thickness of 40 µm, 20 µm above the central plane and 20 µm below the central plane of the spheroid (see **Note 33**).

7. Set up the total recording duration to at least 24-48 h and the intervals' time to 10-20 min (see **Note 34**).

8. Start the time-lapse recording (Fig. 3).

9. The obtained images are processed using Imaris, Volocity or Image J. Obtain cell parameters such as speed by automated or manual cell tracking in the aforementioned software programs. Convert time-lapse image sequences into AVI or MOV format for display in common media players.

   [Fig. 3 near here]

**3.7 Spheroid imaging using multiphoton microscopy and 3D stitching**

1. Visualize the spheroid using a 20x water-dipping objective, lowered into the medium (see **Note 35**).
2. Excite the FUCCI-spheroid using a wavelength of 920 nm (Ti:Sapphire laser) and 1060 nm (OPO).
3. Use a 465 dichroic to remove second-harmonic generation (SHG) signals originating from the Ti:Sapphire laser (see **Note 36**).
4. Use a 520 nm dichroic to split the mKO from the mAG emission, and a bandpass filter 560/40 to further refine the mKO signal and exclude SHG light originating from the OPO.
5. Collect mAG and mKO fluorescence in photomultiplier tubes.
6. Acquire three-dimensional images (x, y, z) of spheroids using the LaVision acquisition software. Use a z spacing of 4 µm, with montaging to cover the entire XY area of the spheroid. Use a z-depth of approximately 600 µm or until the signal fades, in order to image as much of the spheroid depth as possible.
7. Stitch z-stack images in FIJI or ImageJ using the Stich Grid of Images Plugin (16), and perform 3D volume rendering using Volocity software (Fig. 4) (see **Note 37**).

[Fig. 4 near here]

## 4. Notes

1. To start pH should be around 6.8 and should need 2-3 NaOH pellets to reach the right pH and change color to red. Notice that pH might increase slightly when topping up with $H_2O$ to 1 L.

2. It is advisable to prepare at least 20 mL extra in addition to the required volume. Due to its viscosity this solution tends indeed to stick to the surfaces of the container.
3. Coating plates with 1.5% agarose will prevent adhesion of the cells to the bottom of the well and at the same time creates a meniscus that allows grouping of the cells at the center of the well.
4. HEK293T is the embryonic kidney 293 cell line (HEK293) carrying the SV40 T-antigen. The T-antigen makes these cells highly transfectable with vectors carrying the SV40 origin of replication resulting in high viral titers.
5. Add the 2× HeBS drop-wise to the $CaCl_2$/plasmid DNA solution, to achieve optimal calcium-phosphate/DNA precipitate.
6. Gloves and lab coat must be used when working with lentiviral vectors. The transduction must be carried out in a PC2 laboratory equipped with a certified Class II Biosafety cabinet and a tissue culture incubator. The buckets in the centrifuge must be equipped with aerosol-tight covers. Decontaminate the surface of the Biosafety cabinet with 10% bleach at the end of the session.
7. Lentiviral particles can be used fresh, or stored at -80˚C. After thawing and re-freezing, there will be a loss of virus potency.
8. The number of cells to be seeded depends on the cell line used.
9. This step is very important as actively dividing cells give a higher transduction rate than non-dividing cells.
10. Low cell confluence is desired to allow growth for 2 days without splitting.

11. Remember to perform also the single color and the mock transduction as later flow cytometry sorting will be performed for which single color signal compensation is required.
12. Calculation of the virus MOI is not required as expression levels of each construct can be measured by flow cytometry and used for sorting to achieve comparable fluorescence intensity of the FUCCI fluorophores.
13. This is important because confluent cells arrest in $G_1$ and accumulate Cdt1. This will result in stronger intensity of the red fluorescence compared to actively dividing cells that pass through $G_1$.
14. It is possible that no cell is visible at this stage.
15. Usually, cells grow close to the edge of the wells. Two cells close together are likely a single cell clone. Two cells far apart within the well are likely two independent clones and should therefore be disregarded.
16. This procedure needs to be performed quickly in order to prevent hardening of the agarose before it has been dispensed in the wells. Use a multichannel pipette and change tips between each 96-well plate (if preparing multiple plates).
17. In order to facilitate easier cell tracking, untransduced parental cells (non-fluorescent) may be mixed with FUCCI cells in a ratio of 10:1 or even 20:1 when forming spheroids. This will reduce problems with cell separation in imaging software due to density.
18. It is advisable to use cells that were grown at a density of 80% or lower. We have observed in the past that cells at higher confluency resulted in poor spheroid formation.
19. The cells will initially group in close contact to each other as a non-adherent single layer in the center of the well. Over time they will initiate cell-cell contact and begin to form a

3D structure. Once cell-cell contact is initiated (usually after 24 h), the cells will re-start to proliferate allowing the spheroid to expand.

20. A properly formed spheroid should have a reasonably round and regular shape with a necrotic core observable by phase-contrast microscopy as a darker central zone, although the latter might not be visible in all cell lines. The success of spheroid formation depends on the specific cell lines used to form spheroids as well as on the integrity of the agarose coating, i.e. spheroids can form properly in some well but not in others. Some cell lines require seeding of higher number of wells compared to others in order to obtain the same number of properly formed spheroids.

21. The volumes given here are for 1 mL of collagen solution which is enough to embed 9 spheroids, each in a well of a 96-well plate (100 μL per spheroid plus minimal manipulation-related loss of volume). To embed spheroids in larger wells (48- or 24-well plates), adjust the volumes proportionally to the well's surface area. The number of spheroids embedded per well can also be adjusted accordingly (e.g. 3 spheroids in a well of a 24-well plate), however take into consideration that multiple spheroids seeded in a single well might embed in close contact to each other, preventing/compromising their experimental use.

22. In addition, other cell types such as fibroblasts and/or endothelial cells can be added to the collagen gel to mimic the stroma better. Examples of this technique are outlined in (17-19).

23. All work must be undertaken on ice in order to avoid collagen polymerization, unless otherwise desired, i.e. during and following incubation at 37°C.

24. A normal plastic tissue culture plate may be used - but in order to improve image quality, and if a smaller working distance objective is needed, an imaging plate (either glass or thin plastic bottom) should be used.

25. This is important to prevent contact between the transferred spheroid and the bottom of the well. Contact will allow cells that are part of the spheroids to adhere to the plastic and proliferate as a monolayer on the well's surface.

26. With a pair of scissors, enlarge the opening of the pipette tip by cutting approximately 2-3 mm off the tip. Before use, clean and disinfect the blades of the scissors with 80% ethanol.

27. To successfully aspirate a spheroid, immerse the end of the pipette tip in the supernatant and move as close as possible to the spheroid without touching it, then gently but assertively retract the plunger to generate a fluid flow with which the spheroid will move into the tip. Gently release the spheroid into the tube avoiding to damage it.

28. Remove the majority of the supernatant using a pipette attached to a vacuum pump then carefully remove as much as possible of the remaining supernatant using a manual pipette with a gel-loading tip.

29. In the case of untreated spheroids the green and red fluorescence signals are expected to have similar intensity and their use to locate the spheroid is interchangeable. If the intensity of one of the two fluorescence signals is decreased (e. g. due to drug treatment), the channel for the fluorophore with the strongest intensity should be used to locate the spheroid.

30. The starting size and growth rate of the spheroid, as well as whether visualization of cell invasion is desired, are factors to consider when choosing the magnification. If visualization of cell invasion of a fast growing spheroid is desired, the visualization field

at the start of the experiment should include sufficient empty space surrounding the spheroid accounting for the increase in size of the spheroid as well as cell moving out of the spheroid.

31. The ideal position to monitor cell cycle behavior in FUCCI melanoma spheroids is in the middle of the spheroid, as this allows to observe both the inner arrested zone and the outer cycling layer of cells (based on the specific distribution of sub-compartments of cells with different cell cycle behavior outlined in the introduction paragraph).

32. Due to the limited sample penetration depth of confocal microscopy, it might not be possible to visualize the central plane of certain spheroids without experiencing loss of signal. This depends on the spheroid's size, density as well as other factors. The loss of signal might be uneven throughout the plane and give rise to artifacts. The plane of view should be localized as deep as possible without experiencing loss of signal. This compromise might be adopted where setting the plane of view slightly away from the center of the spheroid still provides the desired information. To confirm the lack of artifacts, the same experiment can be repeated for specific time points where sections of the fixed spheroid (instead of the whole spheroid) are imaged using the same microscopy technique. This method prevents potential artifacts generated by limited imaging penetration depth.

33. Collecting z-stack images allows the creation of a maximum intensity projection image to enhance signal intensity when signal from a single optical slice is too weak. The thickness of the z-stack and the number of optical slices it contains should be adjusted according to spheroid's characteristics and in particular to spheroid size. For instance, in melanoma FUCCI spheroids, an excessive z-stack thickness might result in signal contamination from the outer cycling layer into the inner arrested zone of cells. Removal of the bottom z-slices is therefore necessary for optimal outcome.

34. These factors depend on the time necessary for the phenomenon of interest to be captured and the desired level of details. For monitoring changes in cell cycle behavior using the FUCCI system the total recording duration and intervals' time need to be adjusted according to the cell line's cell cycle time.

35. An inverted multiphoton microscope may be preferable if repeated imaging is to take place, or time lapse imaging. This will avoid potential contamination due to the need to remove the tissue culture plate lid.

36. SHG may also be used to image type I collagen fibers (20,21).

37. Several other imaging software have 3D stitching plugins, and FIJI also has additional stitching plugins. If this FIJI plugin fails, one of the other methods should be tried. An alternative is to start with two tiles that do stitch together, and then to build up the larger image iteratively by gradually adding more tiles. For this method the maximum intensity blending method must be used.

**Acknowledgements**

We thank Prof Meenhard Herlyn, The Wistar Institute, Philadelphia, PA; Prof Keiran Smalley, Moffitt Cancer Center, Tampa, FL; Prof Wolfgang Weninger & Dr Ben Roediger, Centenary Institute, Sydney, NSW; Dr Crystal Tonnessen, UQ Diamantina Institute, Brisbane, QLD, and the imaging facilities of the Centenary and UQ Diamantina Institutes for their contribution to optimizing this protocol over the years. We thank Prof Atsushi Miyawaki, RIKEN, Wako-city, Japan, for providing the FUCCI constructs. N.K.H. is a Cameron fellow of the Melanoma and Skin Cancer Research Institute, Australia. K.A.B. is a fellow of Cancer Institute New South Wales (13/ECF/1-39). The work leading to this protocol was supported by project grants RG 09-08 and RG 13-06 (Cancer Council New

South Wales), 570778 and 1051996 (Priority-driven collaborative cancer research scheme/Cancer Australia/Cure Cancer Australia Foundation), 08/RFG/1-27 (Cancer Institute New South Wales), APP1003637 and APP1084893 (National Health and Medical Research Council).

## 5. References

1. Brandner JM, Haass NK (2013) Melanoma's connections to the tumour microenvironment. Pathology 45 (5):443-452. doi:10.1097/PAT.0b013e328363b3bd

2. Villanueva J, Herlyn M (2008) Melanoma and the tumor microenvironment. Curr Oncol Rep 10 (5):439-446

3. Beaumont KA, Mohana-Kumaran N, Haass NK (2014) Modeling Melanoma In Vitro and In Vivo. Healthcare 2 (1):27-46. doi:10.3390/healthcare2010027

4. Santiago-Walker A, Li L, Haass NK et al. (2009) Melanocytes: from morphology to application. Skin Pharmacol Physiol 22 (2):114-121

5. Smalley KS, Lioni M, Noma K et al. (2008) In vitro three-dimensional tumor microenvironment models for anticancer drug discovery. Expert Opin Drug Discov 3 (1):1-10. doi:10.1517/17460441.3.1.1

6. Wroblewski D, Mijatov B, Mohana-Kumaran N et al. (2013) The BH3-mimetic ABT-737 sensitizes human melanoma cells to apoptosis induced by selective BRAF inhibitors but does not reverse acquired resistance. Carcinogenesis 34 (2):237-247. doi:10.1093/carcin/bgs330

7. Hanahan D, Weinberg RA (2000) The hallmarks of cancer. Cell 100 (1):57-70

8. Hanahan D, Weinberg RA (2011) Hallmarks of cancer: the next generation. Cell 144 (5):646-674

9. Sakaue-Sawano A, Kurokawa H, Morimura T et al. (2008) Visualizing spatiotemporal dynamics of multicellular cell-cycle progression. Cell 132 (3):487-498

10. Haass NK, Beaumont KA, Hill DS et al. (2014) Real-time cell cycle imaging during melanoma growth, invasion, and drug response. Pigment Cell Melanoma Res 27 (5):764-776. doi:10.1111/pcmr.12274

11. Beaumont KA, Hill DS, Daignault SM et al. (2016) Cell cycle phase-specific drug resistance as an escape mechanism of melanoma cells. J Invest Dermatol. doi:10.1016/j.jid.2016.02.805

12. Ravindran Menon D, Das S, Krepler C et al. (2015) A stress-induced early innate response causes multidrug tolerance in melanoma. Oncogene 34 (34):4448-4459. doi:10.1038/onc.2014.372

13. Haass NK (2015) Dynamic tumor heterogeneity in melanoma therapy: how do we address this in a novel model system? Melanoma Manag 2 (2):93-95

14. Beaumont KA, Anfosso A, Ahmed F et al. (2015) Imaging- and Flow Cytometry-based Analysis of Cell Position and the Cell Cycle in 3D Melanoma Spheroids. J Vis Exp 106:e53486. doi:10.3791/53486

15. Smalley KS, Brafford P, Haass NK et al. (2005) Up-regulated expression of zonula occludens protein-1 in human melanoma associates with N-cadherin and contributes to invasion and adhesion. Am J Pathol 166 (5):1541-1554

16. Preibisch S, Saalfeld S, Tomancak P (2009) Globally optimal stitching of tiled 3D microscopic image acquisitions. Bioinformatics 25 (11):1463-1465. doi:10.1093/bioinformatics/btp184

17. Flach EH, Rebecca VW, Herlyn M et al. (2011) Fibroblasts contribute to melanoma tumor growth and drug resistance. Mol Pharm 8 (6):2039-2049. doi:10.1021/mp200421k

18. Haass NK, Sproesser K, Nguyen TK et al. (2008) The mitogen-activated protein/extracellular signal-regulated kinase kinase inhibitor AZD6244 (ARRY-142886) induces growth arrest in melanoma cells and tumor regression when combined with docetaxel. Clin Cancer Res 14 (1):230-239

19. Velazquez OC, Snyder R, Liu ZJ et al. (2002) Fibroblast-dependent differentiation of human microvascular endothelial cells into capillary-like 3-dimensional networks. Faseb J 16 (10):1316-1318

20. Kirkpatrick ND, Hoying JB, Botting SK et al. (2006) In vitro model for endogenous optical signatures of collagen. J Biomed Opt 11 (5):054021. doi:10.1117/1.2360516

21. Tong PL, Qin J, Cooper CL et al. (2013) A quantitative approach to histopathological dissection of elastin-related disorders using multiphoton microscopy. Br J Dermatol 169 (4):869-879. doi:10.1111/bjd.12430

**Figure legends**

**Figure 1.** Spheroid formation: A day-by day schematic illustration of the different stages of spheroid formation and the main steps involved in this procedure.

**Figure 2.** Spheroid embedding: schematic illustrating the main steps involved in the procedure for embedding spheroids in collagen matrix.

**Figure 3.** Confocal extended focus image of a FUCCI-melanoma spheroid (1:10 FUCCI-C8161 cells to wt-C8161 cells, from 0-13 h after collagen embedding. The top few z-slices were removed to reveal the red G1-arrested cells inside the spheroid. White arrows indicate a single invading cell tracked over time. Note the cell cycle change of the invading cell from G1 (red) to S/G2/M (green). Scale bar, 100 μm.

**Figure 4.** 3D rendering of a multiphoton microscopy image z-stack of a FUCCI-melanoma spheroid (C8161) 24 h after collagen implantation.

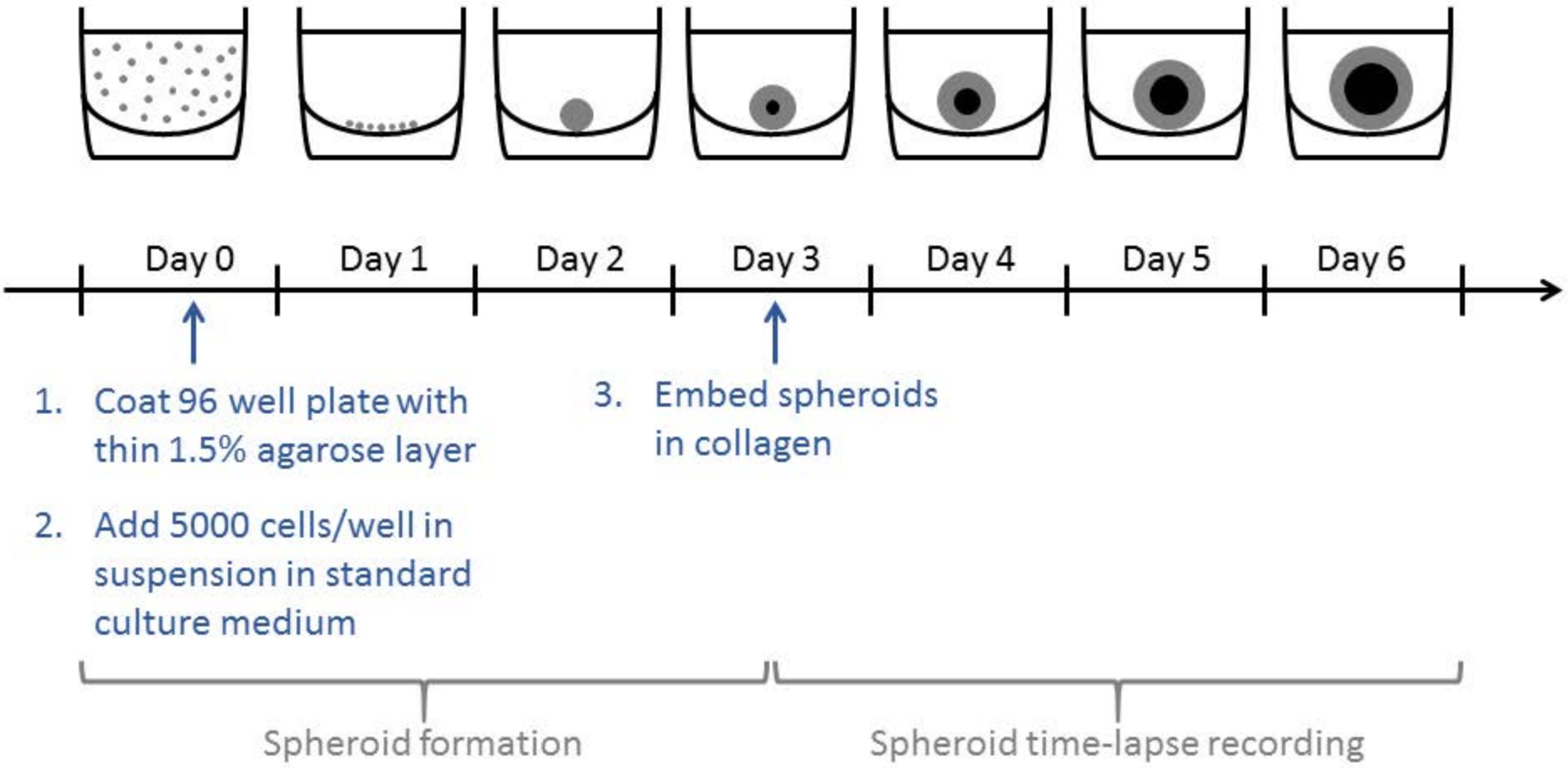
Day 0
Day 1
Day 2
Day 3
Day 4
Day 5
Day 6
1. Coat 96 well plate with thin 1.5% agarose layer
2. Add 5000 cells/well in suspension in standard culture medium
3. Embed spheroids in collagen
Spheroid formation
Spheroid time-lapse recording

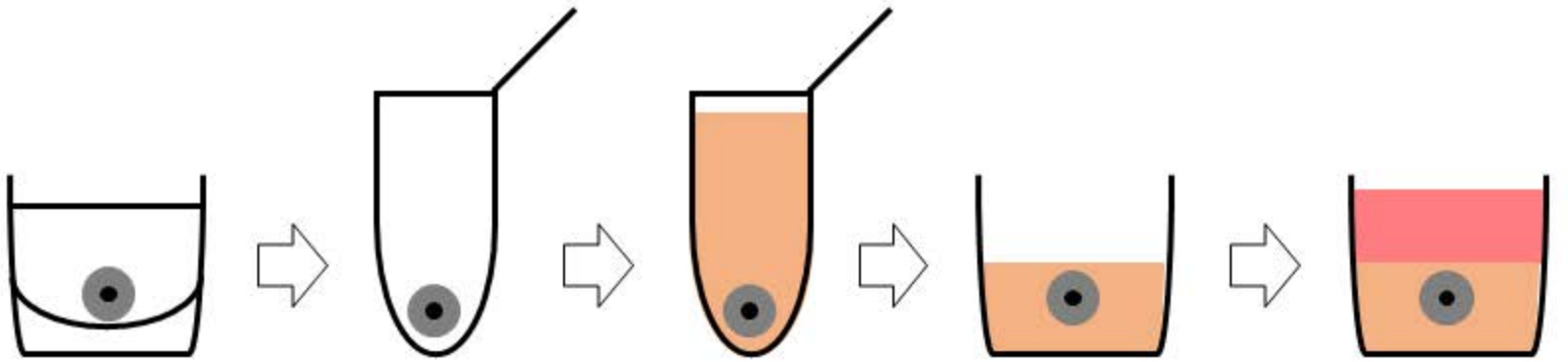

Transfer spheroid to tube, let it sink and remove supernatant

Resuspend spheroid in collagen solution

Transfer spheroid into 96 well plate pre-coated with thin layer of collagen mix

Add culture medium once collagen mix has polymerised

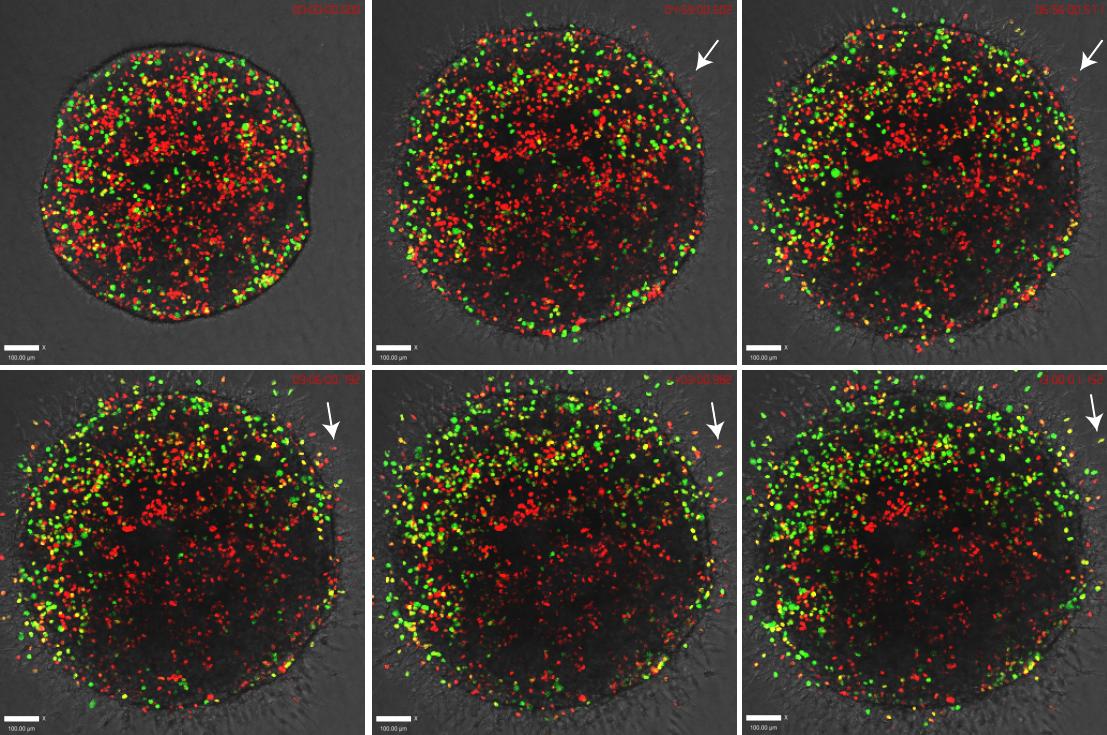
00:00:00.000
04:59:00.502
05:58:00.511
03:06:00.192
03:00.986
100.00 µm